



Influence of differentially heated horizontal walls on the streaming shape and velocity in a standing wave resonator[☆]

Majid Nabavi^{*}, Kamran Siddiqui, Javad Dargahi

Department of Mechanical and Industrial Engineering, Concordia University, 1455 de Maisonneuve Blvd. West, Montreal, Quebec, Canada H3G 1M8

ARTICLE INFO

Available online 18 July 2008

Keywords:

Acoustic streaming
Particle image velocimetry
Experimental analysis
Temperature gradient

ABSTRACT

Influence of differentially heated horizontal walls on shape and amplitude of acoustic streaming velocity field inside a gas-filled rectangular enclosure subject to acoustic standing wave are experimentally investigated. The synchronized particle image velocimetry (PIV) technique has been used to measure the streaming velocity fields. The results show that the temperature difference between the top and the bottom walls deforms the symmetric streaming vortices to the asymmetric ones. As the temperature difference increases, the amplitude of streaming velocity increases.

© 2008 Elsevier Ltd. All rights reserved.

1. Introduction

One of the important nonlinear phenomena in the field of acoustics is the acoustic streaming, a stationary fluid flow generated by sound. The interaction between the acoustic waves in a viscous fluid and the solid wall is responsible for this phenomenon. The classical streaming structure predicted by Rayleigh theory, is typically comprised of two streaming vortices per quarter-wavelength of the acoustic wave which are symmetric about the channel center line. The phenomenon of acoustic streaming has been extensively studied using the analytical [1], numerical [2,3,4] and experimental [5,6] methods.

The influence of the axial temperature gradient (i.e. the temperature gradient in the direction of the acoustic wave propagation) on acoustic streaming has been extensively studied analytically, numerically and experimentally. Rott [7] derived a simplified analytical formula for the acoustic streaming including the effect of the variable tube wall temperature. Aktas et al. [8] numerically investigated thermal convection in a 2-D resonator. In their model, the left and right sidewalls were kept at different temperatures, while the top and the bottom walls were kept insulated. They reported that the influence of mechanically-induced periodic oscillations on the heat transfer characteristics of the system is significant only in the presence of steady streaming flows. Thompson et al. [9] experimentally investigated the influence of axial temperature gradient on the behavior of the streaming flow. They observed that as the magnitude of the axial temperature gradient increases, the shape of streaming vortices becomes distorted.

Unlike the axial temperature gradient, the influence of transverse temperature gradient (i.e. the temperature gradient orthogonal to the direction of acoustic wave propagation) on acoustic streaming is scarcely investigated. Very recently, only one study has numerically investigated this behavior [10]. They considered the temperature dependent conductivity and viscosity in their model and conducted simulations at top-bottom wall temperature difference of 0, 20 and 60 °C. At 20 and 60 °C, they found that the classical two symmetric streaming vortices are distorted to one vortex. However, they did not study the transition behavior of streaming vortices due to the gradual increase in the temperature gradient. Furthermore, they did not provide any validation of their numerical model.

In the present study, we experimentally investigated the influence of transverse temperature gradient on the streaming patterns. The synchronized particle image velocimetry (PIV) technique is used to measure the streaming velocity fields for isothermal condition and differentially heated horizontal walls. To the best of authors' knowledge, this is the first experimental investigation of the streaming patterns in the presence of transverse temperature gradients.

2. Experimental setup

The experimental setup used in this study is shown in Fig. 1. The acoustic chamber is a Plexiglas channel of square cross-section. The channel is 105 cm long with the inner cross-section of 4 cm × 4 cm. The walls of the channel are 10 mm thick. The two-dimensional streaming velocity fields inside the channel are measured using synchronized PIV technique. A New Wave Research 120 mJ Nd:YAG laser is used as a light source for the PIV measurements. A digital 2 Megapixel progressive scan CCD camera (JAI CV-M2) with the resolution of 1600 × 1200 pixels is used to image the flow. The camera is connected to a PC equipped with a frame grabber (DVR Express, IO Industries, London, ON, Canada) that acquired 8 bit images at a rate of 30 Hz. A

[☆] Communicated by W.J. Minkowycz.

^{*} Corresponding author.

E-mail address: m_nabav@encs.concordia.ca (M. Nabavi).

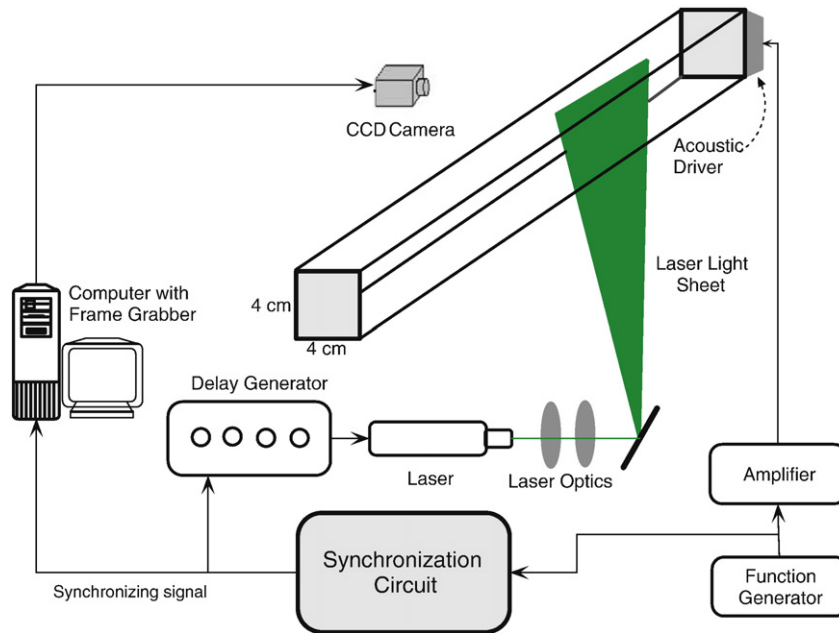


Fig. 1. Schematic of the experimental setup.

four-channel digital delay generator (555-4C, Berkeley Nucleonics Corporation, San Rafael CA) is used to control the timing of the laser pulses. BIS(2-ETHYLHEXYL) SEBACATE mist with the mean diameter of $0.5 \mu\text{m}$ is used as the tracer particles. An aerosol generator (Lavisson Inc., Ypsilanti MI) is used to generate the mist. The acoustic pressure is measured by a condenser microphone cartridge Model 377A10 PCB Piezotronics. A special loudspeaker driver is used to excite the acoustic standing wave inside the tube. The driver has the maximum power of 200 W. A function generator is used to generate the sinusoidal wave. The signal from the function generator is amplified by a 220-W amplifier. The loudspeaker is driven by this amplified signal (see Fig. 1).

The basic principal of the synchronized PIV technique is shown in Fig. 2. Consider the image taken at time t_1 in Fig. 2 as the first image and the image taken at time t_2 as the second image, with the time separation of $t_2 - t_1$. The cross-correlation of this image pair provides the acoustic velocity field at time t_1 . Now, consider the image taken at time t_1 as the first image and the image taken at time t_3 as the second image, with the time separation of $t_3 - t_1$. Since the images acquired at t_1 and t_3 are exactly at the same phase, the acoustic velocity components at these times will be the same, therefore, the particle shift between these two images will only be due to streaming velocity. Thus, the cross-correlation of this image pair will provide the streaming velocity field at time t_1 (see Nabavi et al. [11] for more

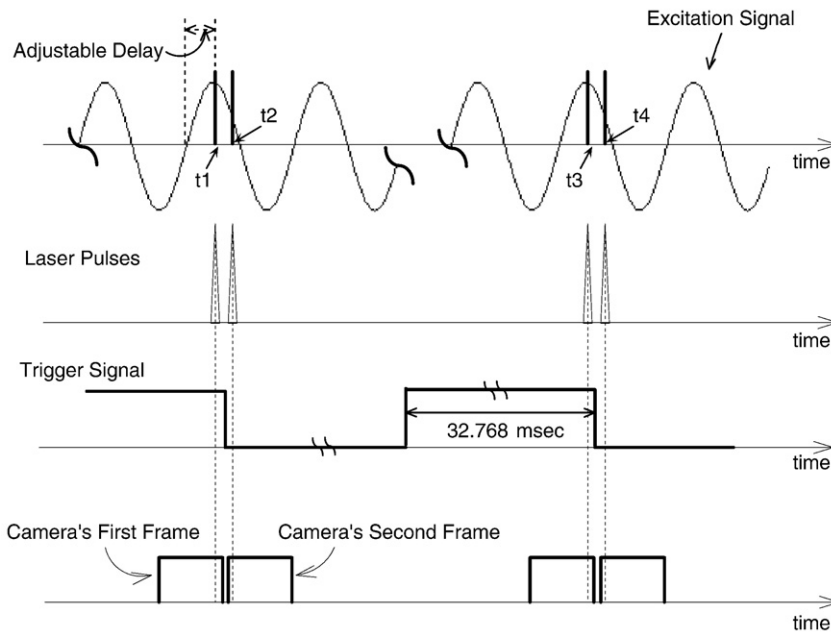


Fig. 2. The triggering sequence that shows the simultaneous measurement of the acoustic and streaming velocity fields at a particular phase of the excitation signal. t_1 and t_2 correspond to the times at which the first and second images of an image pair are captured. t_3 and t_4 are the times associated with the first and second images of the consecutive image pair.

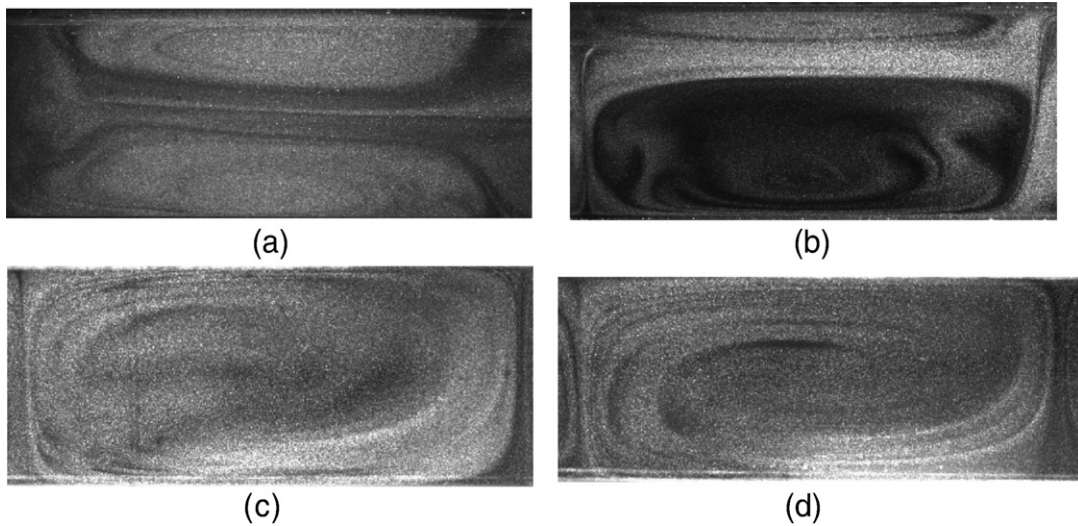


Fig. 3. Sample PIV images in the quarter-wavelength region of the resonator at (a) $\Delta T=0$ °C, (b) $\Delta T=0.3$ °C, (c) $\Delta T=0.8$ °C, and (d) $\Delta T=3$ °C.

details of the synchronized PIV technique). Trigger signal (TS) in Fig. 2 is used to trigger both laser and CCD camera of the PIV system. That is, both the laser and the camera are synchronized with the excitation signal via TS. The synchronization sequence for the excitation signal, laser pulses, camera frames and trigger signal is also shown in Fig. 2.

In the present experiments, the driver frequency is set equal to $f=976$ Hz resulting in the formation of three complete standing waves inside the channel. The camera field of view is set equal to 10.5 cm in horizontal and 8 cm in vertical that allows to capture the streaming velocity field in the quarter-wavelength region. The maximum vibration displacement of the acoustic driver is set equal to 65 μm and the corresponding maximum acoustic pressure is 775 Pa. Four different thermal boundary conditions are considered which are $\Delta T=0$

(isothermal), $\Delta T=0.3$ °C, $\Delta T=0.8$ °C, and $\Delta T=3$ °C, where ΔT is the temperature difference between the bottom and top walls (i.e. $\Delta T=T_{\text{bottom}}-T_{\text{top}}$).

To achieve isothermal boundary condition, the resonator is placed inside a large water tank of dimensions 50×50×90 cm. To achieve differentially heated horizontal walls, the resonator is placed on top of an aluminum plate (150×10×2 cm). The surface of the aluminum plate of the test section was coated black with high temperature paint to minimize the laser reflection. Two electric strip heaters are attached to the bottom of the aluminum plate. Constant temperature of the aluminum plate is maintained by using a PID controller. Five thermocouples were placed along the aluminum plate to act as a feedback to the PID controller.

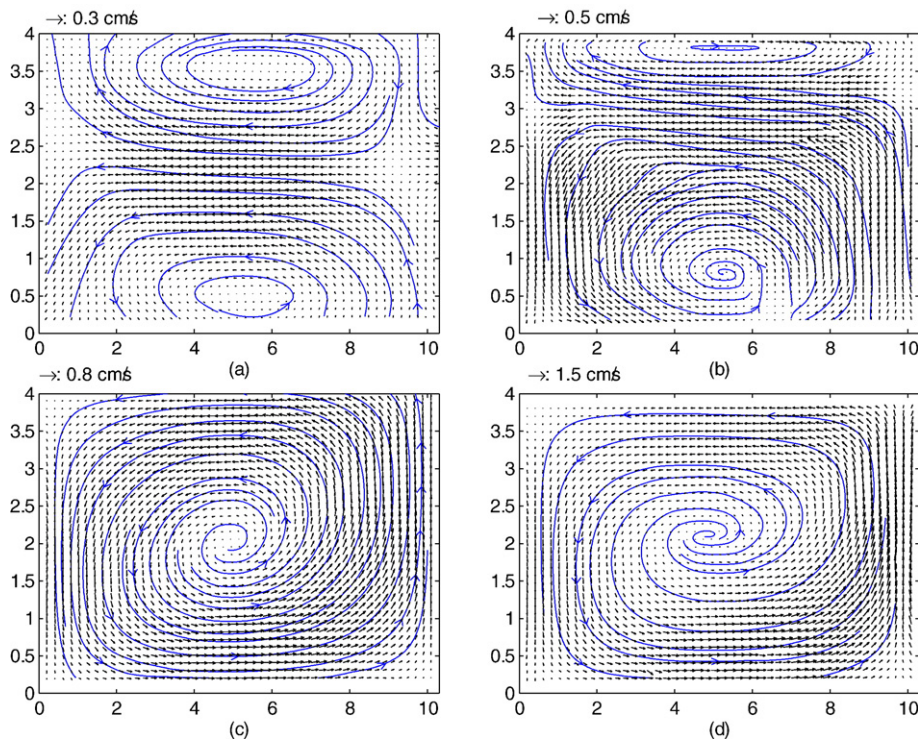


Fig. 4. The streaming velocity fields correspond to the PIV images shown in Fig. 3, (a) $\Delta T=0$ °C, (b) $\Delta T=0.3$ °C, (c) $\Delta T=0.8$ °C, and (d) $\Delta T=3$ °C. Horizontal axis is the axial location in cm. Vertical axis is the transverse location in cm.

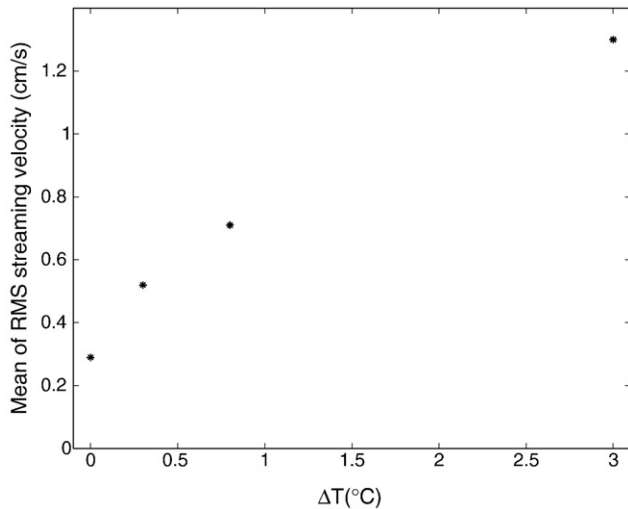


Fig. 5. The mean RMS axial streaming velocities along the resonator versus ΔT .

The characteristic response time of the seed particles is used as an estimate of the accuracy of the acoustic velocity measurements using PIV. The characteristic response time of the seed particles is computed by $T_p = u_T/g$, where T_p is the particle response time, u_T is the particle terminal velocity and g is the acceleration due to gravity [12]. The terminal velocity is computed by $u_T = (\gamma - 1)D^2g/18\nu$, where D is the diameter of the tracer particles, ν is the kinematic viscosity of the fluid and γ is the ratio of the density of particle to the density of fluid [13]. Using the above equations, for $D = 0.5 \mu\text{m}$ and $u_T = 6.5 \mu\text{m/s}$, the particle response time is found to be $T_p = 0.67 \mu\text{s}$. For the driver frequency of 976 Hz, the particle response is more than 1500 times faster than the wave period. Thus, we conclude that the tracer particles accurately follow the flow.

For PIV cross-correlation, the size of the interrogation region is set equal to 32×32 pixels and the size of the search region is set equal to 64×64 pixels. A 50% window overlap is used in order to increase the nominal resolution of the velocity field to 16×16 pixels. A three-point Gaussian sub-pixel fit scheme is used to obtain the correlation peak with sub-pixel accuracy. The spurious velocity vectors are detected and then corrected using a local median test.

3. Results and discussions

A sample PIV image for each of the four cases is shown in Fig. 3. The corresponding streaming flow patterns are shown in Fig. 4. The streamlines are also depicted in Fig. 4 for better flow visualization. For isothermal case (Fig. 4a), two streaming vortices per quarter-wavelength of the acoustic wave are observed which are symmetric about the channel center line. As the bottom wall is slightly heated ($\Delta T = 0.3 \text{ }^\circ\text{C}$, Fig. 4b), the bottom vortex vertically expands while the top vortex vertically contracts. As the temperature difference further increases ($\Delta T = 0.8 \text{ }^\circ\text{C}$ Fig. 4c), the top vortex completely disappears. Once the top vortex disappeared, a further increase in ΔT has no significant effect on the streaming flow structure. These results provide the first experimental evidence of the influence of transverse temperature gradient on the transitional behavior of the streaming flow structure. The results also indicate that the transition could occur at small values of ΔT .

The influence of the transverse temperature gradient on the magnitude of the steaming velocity field is quantified in terms of the mean root-mean-square (RMS) axial streaming velocities. The results are plotted in Fig. 5 for all cases. The plot shows that as ΔT increases, the streaming velocity magnitude increases. The higher temperature at the bottom wall induces convective motion in the flow domain. Fig. 4 shows that once the transition occurred, the streaming patterns remain the same (for $\Delta T = 0.8 \text{ }^\circ\text{C}$ and $3 \text{ }^\circ\text{C}$), however, as shown in Fig. 5, the streaming velocity magnitude increases by 80%. These results indicate that the convective currents are aligned with the streaming flow patterns.

4. Conclusion

Influence of differentially heated horizontal walls on the shape and amplitude of acoustic streaming velocity field are investigated experimentally using the synchronized PIV technique. The results indicate that the temperature difference between the top and bottom walls deforms the symmetric streaming vortices to the asymmetric form. As the temperature difference increases, the amplitude of streaming velocity increases.

Acknowledgements

This research is funded by the grants from Natural Science and Engineering Research Council of Canada (NSERC) and Concordia University.

References

- [1] M.F. Hamilton, Y.A. Ilinskii, E.A. Zabolotskaya, Acoustic streaming generated by standing waves in two-dimensional channel of arbitrary width, *J. Acoust. Soc. Am.* 113 (2003) 153–160.
- [2] M. Kawahashi, M. Arakawa, Nonlinear phenomena induced by finite amplitude oscillation of air-column in closed duct, *JSME* 39 (1996) 280–286.
- [3] M.K. Aktas, B. Farouk, Numerical simulation of acoustic streaming generated by finite-amplitude resonant oscillations in an enclosure, *J. Acoust. Soc. Am.* 116 (2004) 2822–2831.
- [4] Q. Wan, A.V. Kuznetsov, Investigation of the acoustic streaming in a rectangular cavity induced by the vibration of its lid, *Int. Commun. Heat Mass Transf.* 31 (2004) 467–476.
- [5] M.W. Thompson, A.A. Atchley, Simultaneous measurement of acoustic and streaming velocities in a standing wave using laser Doppler anemometry, *J. Acoust. Soc. Am.* 117 (2005) 1828–1838.
- [6] S. Moreau, S.H. Bailliet, J.C. Valiere, Measurements of inner and outer streaming vortices in a standing waveguide using laser Doppler anemometry, *J. Acoust. Soc. Am.* 123 (2008) 640–647.
- [7] N. Rott, The influence of heat conduction on acoustic streaming, *J. Appl. Math. Phys.* 25 (1974) 417–421.
- [8] M.K. Aktas, B. Farouk, Heat transfer enhancement by acoustic streaming in an enclosure, *J. Heat Transfer* 127 (2005) 1313–1321.
- [9] M.W. Thompson, A.A. Atchley, M.J. Maccarone, Influences of temperature gradient and flow inertia on acoustic streaming in a standing wave, *J. Acoust. Soc. Am.* 117 (2005) 1839–1849.
- [10] Y. Lin, B. Farouk, Heat transfer in a rectangular chamber with differentially heated horizontal walls: effects of a vibrating sidewall, *Int. J. Heat Mass Transf.* 51 (2008) 3179–3189.
- [11] M. Nabavi, K. Siddiqui, J. Dargahi, Simultaneous measurement of acoustic and streaming velocities using synchronized PIV technique, *Meas. Sci. Technol.* 18 (2007) 1811–1817.
- [12] W.H. Snyder, J.L. Lumley, Some measurements of particle velocity autocorrelation functions in a turbulent flow, *J. Fluid Mech.* 48 (1971) 41–71.
- [13] D.A. Siegel, A.J. Plueddemann, The motion of a solid sphere in an oscillating flow: an evaluation of remotely sensed Doppler velocity estimates in the sea, *J. Atmos. Ocean. Technol.* 8 (1991) 296–304.